



Fixed-bed adsorption of metal ions from aqueous solution on polyethyleneimine-impregnated palm shell activated carbon

Chun Yang Yin^{a,*}, Mohd Kheireddine Aroua^b, Wan Mohd Ashri Wan Daud^b

^a Faculty of Chemical Engineering, Universiti Teknologi MARA, 40450 Shah Alam, Selangor, Malaysia

^b Department of Chemical Engineering, Faculty of Engineering, University of Malaya, 50603 Kuala Lumpur, Malaysia

ARTICLE INFO

Article history:

Received 19 October 2007

Received in revised form 7 July 2008

Accepted 13 July 2008

Keywords:

Polyethyleneimine-impregnated activated carbon

Copper

Nickel

Fixed-bed adsorption

Modelling

ABSTRACT

Fixed-bed adsorption studies with virgin and polyethyleneimine (PEI)-impregnated palm shell activated carbon (AC) as a media for the removal of single Ni²⁺ or Cu²⁺ ions from aqueous solution were conducted. The studies were conducted in a vertical down flow Perspex column with influent pH at 5 with either Ni²⁺ or Cu²⁺ had an influent concentration of 1 mmol/L. The adsorption data were fitted to three-well-established fixed-bed adsorption models, namely, bed-depth-service-time (BDST), Thomas and Yoon–Nelson models. It was observed that PEI impregnation at 8.41 wt% had increased the breakthrough volume and service time of AC by factors of 2.1 (Cu²⁺) and 1.6 (Ni²⁺) as compared to virgin AC. For Cu²⁺ adsorption, the modelled BDST, Thomas and Yoon–Nelson curves were in very good agreement with the experimental curves while it was conversely true for Ni²⁺ adsorption.

© 2008 Elsevier B.V. All rights reserved.

1. Introduction

The presence of highly concentrated toxic metals such as lead, cadmium, copper, nickel, chromium and mercury in industrial wastewaters is a great environmental concern since they exert detrimental impacts on the surrounding ecological systems as well as pose public health concerns. These wastewaters generally originated from industries such as metal plating, paint and metal finishing. There are numerous effective treatment techniques for these metal-laden wastewaters such as precipitation, adsorption, ion exchange and reverse osmosis [1,2]. Among these, precipitation is often deemed as the most economical means while reverse osmosis is relatively the most expensive. Precipitation, however, does have its shortcomings as large amount of sludge can be produced which necessitate further treatment. Adsorption using activated carbon (AC) is also an established means and it is often used in the tertiary wastewater treatment stage for polishing incoming influent before final discharge into water bodies. Recent studies have focused on the modification of activated carbon to enhance metal affinity and/or increase the activated carbon's affinity towards a certain metal species. One frequently used modification technique was via wet oxidization using strong acid solutions such as hydrofluoric

[3], nitric [4,5] and hydrochloric [6] acids which are used to increase metal affinity. In addition to wet oxidation, other researchers also impregnated activated carbon with other substances for fixed-bed metal ion adsorption.

Monser and Adhoum [2] studied the adsorption of copper(II), zinc(II) and chromium(VI) ions onto the surface of fixed-bed activated carbon impregnated with tetrabutyl ammonium (TBA) and sodium diethyl dithiocarbamate (SDDC). They reported that the TBA-immobilized activated carbon had an effective removal capacity of approximately 5 times that of the virgin activated carbon while the SDDC-immobilized activated carbon had an effective removal capacity for copper(II) (4 times), zinc(II) (4 times), chromium(VI) (2 times) greater than the virgin activated carbon. Recently, Mugisidi et al. [7] modified activated carbon produced from coconut shell with sodium acetate at concentrations of 10% and 15%, and used it in a fixed-bed column to study the adsorption of copper ions. Their results showed that the highest adsorption capacity was found for AC modified with 15% sodium acetate by 2.2 times compared to virgin AC.

In our previous study, palm shell AC was impregnated with polyethyleneimine (PEI) [8] in order to increase its metal affinity. PEI is a well-recognized polymer with high metal complexation capability. It was shown PEI-impregnated AC (as compared to virgin AC) significantly increased the maximum batch single adsorption capacity for Cd²⁺ by 96%. The positive outcome of the study justifies further research especially in terms of continuous fixed-bed adsorption. Issabayeva [9] was the first researcher to conduct

* Corresponding author. Tel.: +60 3 55436348; fax: +60 3 55436300.

E-mail addresses: yinyang@salam.uitm.edu.my, yinyang@streamyx.com (C.Y. Yin).

fixed-bed column studies using palm shell AC for metal ion adsorption. However, there is no known study done using PEI-impregnated AC as bed media for adsorption of metal ions. The main objectives of this study were (a) to evaluate the effect of PEI impregnation of palm shell AC on its fixed-bed adsorption capacity for the removal of Ni^{2+} or Cu^{2+} ions from aqueous solution and (b) to fit the adsorption data to several well-established fixed-bed adsorption models. Nickel and copper ions were selected in this study because they are commonly present in wastewater effluent in a variety of industries and they are among the most toxic metals.

2. Experimental

2.1. Preparation and textural characterization of activated carbon samples

AC used in the study was oil palm shell-based produced by physical activation process with steam as the activating agent. It was supplied by Bravo Green Sdn Bhd (Malaysia). The activated carbon was sieved to sizes range from 710 to 850 μm , washed with deionized water ($>18 \text{ M}\Omega \text{ cm}$) to remove fines and dirt, oven dried at 105°C for a day before impregnation process. Low molecular weight PEI with average molecular number of 423 obtained from Sigma–Aldrich (catalog no.: 468533) was used as an impregnation agent. The impregnation process was similar to a batch adsorption process conducted in a previous study [8]. In this study, however, the initial concentrations of PEI for the process were fixed at 5 and 8 g/L which subsequently yielded 8.41 and 16.68 wt% PEI/AC. These concentrations were chosen as it was determined in a preliminary study that these impregnation percentages provided the highest metal ion batch adsorption capacities. Textural characteristics of AC samples were determined from N_2 adsorption isotherm at 77 K using the N_2 adsorption isotherm using Quantachrome Autosorb-1 system. Prior to analysis, the samples were degassed at 120°C for at least 24 h.

2.2. Fixed-bed adsorption

Fixed-bed adsorption studies (single metal component) were conducted in a 2 cm i.d., 9-cm length vertical down flow Perspex column packed with either virgin or PEI-impregnated AC (fixed-bed packing: i.d. = 2 cm; height = 6 cm). The column-to-particle diameter ratio was approximately 23, considered sufficient to minimize wall effect. Nylon felts were placed on the top and bottom of the fixed bed to prevent loss of the activated carbon. The experimental setup is illustrated in Fig. 1. The influent feed flow rate was maintained at either 5, 10 or 15 mL/min using Cole Palmer Masterflex peristaltic pump with size 14-silicon tube. The influent pH was fixed at 5 with either Ni^{2+} or Cu^{2+} had an influent concentration of 1 mmol/L. This influent pH value was selected since Malaysian industrial wastewaters primarily exist at pH 3 or 5 [10]. Solutions were prepared by dissolving metal perchlorate salt at a known concentration in 0.15 M sodium perchlorate to obtain a stock solution as specified in our previous study [8]. Perchlorate metal salt was chosen due to its very poor complexation tendencies at low pH. In order to facilitate a more focused discussion and brevity, only fixed-bed adsorption for influent at pH 5 was studied here as our previous study [8] showed that adsorption trend of PEI-impregnated AC at solution pH 5 was similar to pH 3, albeit adsorption capacity at the former pH was considerably higher. Cyberscan 510 pH meter was used for all pH measurements in this study and metal concentrations before and after adsorption were determined via Varian Liberty 220 ICP-AES.

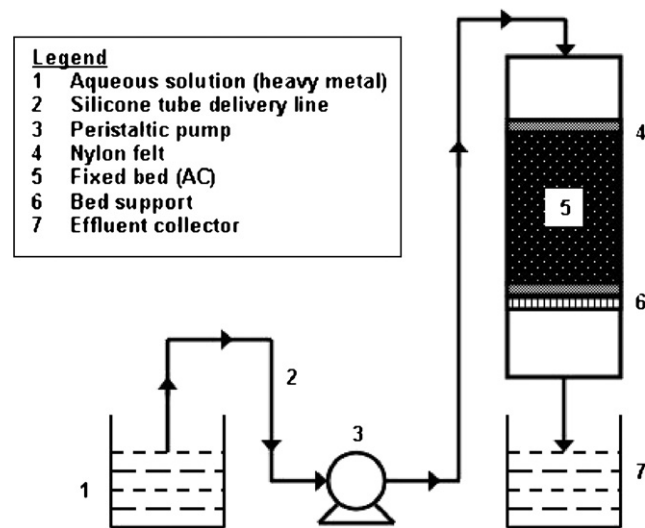


Fig. 1. Experimental setup for the study.

3. Results and discussion

3.1. Textural characterization

The textural characteristics of virgin and PEI-impregnated AC are shown in Table 1. The BET surface area of the AC decreases with the increase of wt% of PEI impregnated. The molecular size (in terms of diameter) of PEI is estimated to be 0.82 nm by using “radius of inertia” equation shown by Schurer et al. [11]. This implies occurrence of pore clogging due to bulk filling of PEI molecules into micropores since the PEI molecules are smaller than micropores (2 nm). The virgin AC is almost entirely micropores while PEI impregnation appears to increase the percentage of mesopores in the AC.

3.2. Fixed-bed adsorption

Fig. 2 shows the effect of PEI-impregnation on effluent pH. A similar trend is exhibited throughout the volume throughput for all the fixed-bed adsorption studies in which pH increases drastically from influent pH of 5 to effluent pH higher than 10 initially before gradually decreases to pH less than 6 and approaching towards influent pH. Studies on fixed-bed adsorption of metal ions onto fixed-bed AC columns conducted by Chen and Wang [1] and Chen et al. [12] also yielded similar effluent pH trend. This probably caused by the presence of high availability of adsorption sites (unsaturated) on AC at initial volume throughput which facilitates high adsorption rates of both metal and H^+ ions. At initial volume throughput, more H^+ ions are adsorbed on the surface of AC and the pH of bulk solution increases as a result of increased percentage of OH^- ions as compared to H^+ ions. As the experiment progresses, adsorption sites on AC are getting relatively saturated resulting in reduced H^+ adsorption and lower effluent pH.

Generally, the effluent pH for both 8.41 and 16.68 wt% PEI/AC are higher than for virgin. This is due to the presence of amine groups

Table 1
Textural characteristics of AC samples

| | Virgin | 8.41 wt% PEI/AC | 16.68 wt% PEI/AC |
|--|--------|-----------------|------------------|
| BET surface area (m^2/g) | 1027 | 532 | 128 |
| Total pore volume (cm^3/g) | 0.45 | 0.27 | 0.10 |
| Average pore diameter (nm) | 2.02 | 1.75 | 3.02 |
| % microporosity (approximate) | 96.58 | 87.94 | 63.87 |

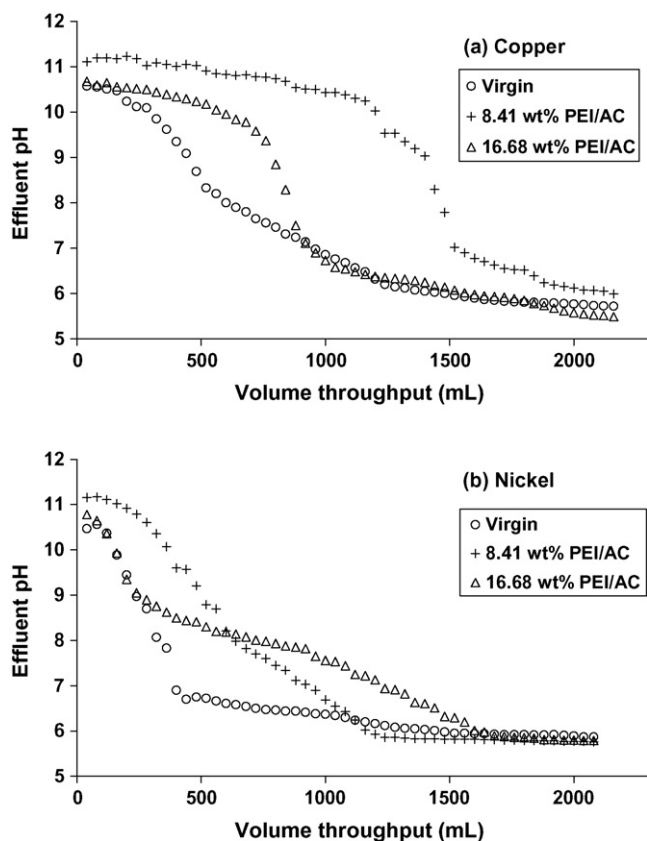


Fig. 2. Effect of PEI-impregnation on effluent pH for (a) Cu^{2+} and (b) Ni^{2+} .

attached on the surface of PEI/AC which provided increased basicity. However, at the volume throughput higher than 2000 mL, the effluent pH values for all AC samples appear to be almost similar. It is interesting to note that effluent pH for adsorption of Cu^{2+} on 8.41 and 16.68 wt% PEI/AC decrease gradually before sudden pH decrease occurs at approximate volume throughputs of 750 and 1250 mL, respectively. This implies that H^+ adsorption is still significant before the aforesaid volume throughputs which further suggests that there are still many free adsorption sites on AC. This is an early indication that PEI impregnation has increased the ion adsorption capacity of AC.

Fig. 3 shows the breakthrough curves for adsorption of Cu^{2+} and Ni^{2+} virgin and PEI-impregnated AC at influent pH 5 and flow rate 5 mL/min. These curves were plotted in accordance with normalized effluent single metal ion concentration ($C_{\text{effluent}}/C_{\text{influent}}$) against volume throughput (mL). The breakthrough curves show a typical “S” shape profile indicating fixed-bed adsorption for adsorbate of smaller molecular weight and simple structure [13]. It is interesting to note that the breakthrough curves for Cu^{2+} have shifted from right (virgin AC) to left (8.41 and 16.68 wt% PEI/AC) as a result of PEI impregnation. The breakthrough point is defined as the phenomenon when the effluent concentration from the column is approximately 3–5% of the influent concentration [14]. The breakthrough points for this study are quite noticeable as indicated by sudden increase in $C_{\text{effluent}}/C_{\text{influent}}$ for a particular breakthrough curve. Breakthrough points for Cu^{2+} occur at volume throughputs of approximately 680 mL (virgin), 1440 mL (8.41 wt% PEI/AC) and 880 mL (16.68 wt% PEI/AC) while for Ni^{2+} adsorption, breakthrough points occur at approximately 200 mL (virgin), 320 mL (8.41 wt% PEI/AC) and 160 mL (16.68 wt% PEI/AC). As such, 8.41 wt% PEI/AC fixed bed is much more efficient in removing Cu^{2+} and Ni^{2+} as compared to virgin and 16.68 wt% PEI/AC. PEI impregnation at 8.41 wt%

has increased the breakthrough volume and service time of AC by factors of 2.1 (Cu^{2+}) and 1.6 (Ni^{2+}). It is also surmised that both virgin and PEI-impregnated AC are more effective in removing Cu^{2+} than Ni^{2+} .

The increases of metal adsorption capacities due to the impregnation of PEI are attributed to increased metal complexation capabilities and improved site coordination for adsorption of metal ions as a result of presence of PEI. Even though PEI impregnation reduces the BET surface area by approximately 49%, it is surmised that the abovementioned favorable effects provided by PEI impregnation render the detrimental effect of surface area reduction insignificant.

3.3. Effect of influent flow rate

Fig. 4 shows the effect of influent flow rate on effluent pH. For Cu^{2+} adsorption, pH increases drastically from influent pH of 5 to effluent pH higher than 10 initially before gradually decreasing to pH less than 6 and approaching towards influent pH. However, it is observed that the effluent pH for cases of Ni^{2+} adsorption at flow rates of 10 and 15 mL/min reach values of about 8.5 instead of values lesser than 6. This is most probably due to the comparatively lower stability of Ni–PEI complex as compared to Cu–PEI complex [15]. It is deemed that this factor induces relatively lower Ni^{2+} complexation ability with PEI resulting in increased competition for adsorption sites from H^+ ions from the bulk solution. This is further exacerbated by increased flow rate at 10 and 15 mL/min since the residence time for Ni^{2+} ions is further reduced. As such, more H^+ ions are adsorbed (complexed) on surface of 8.41 wt% PEI/AC resulting in loss of acidity of the bulk solution. This is also observed in the study conducted by Chen et al. [12]. They elucidated that this anomaly was due to the change in the solution chemistry, which

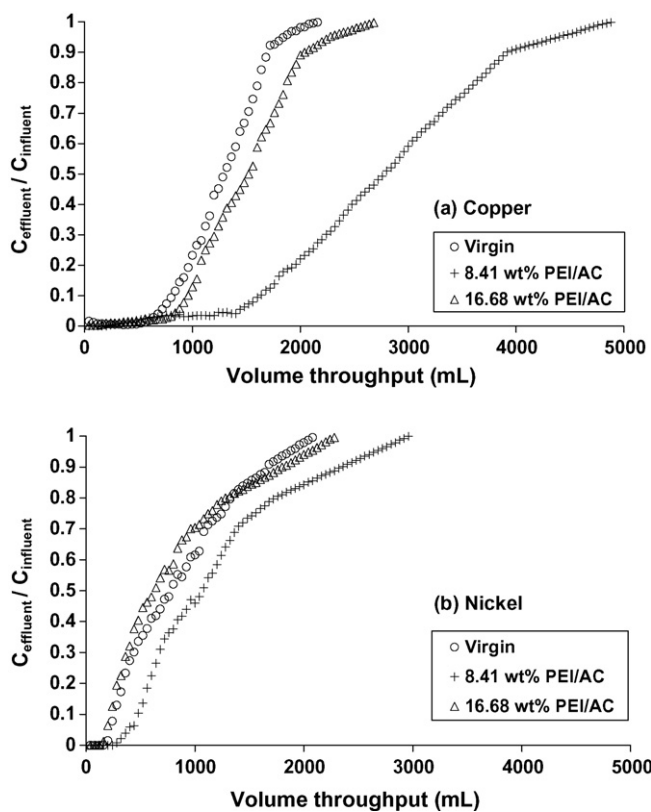


Fig. 3. Breakthrough curves of adsorption of (a) Cu^{2+} and (b) Ni^{2+} on virgin and PEI-impregnated AC at influent pH 5 and flow rate 5 mL/min.

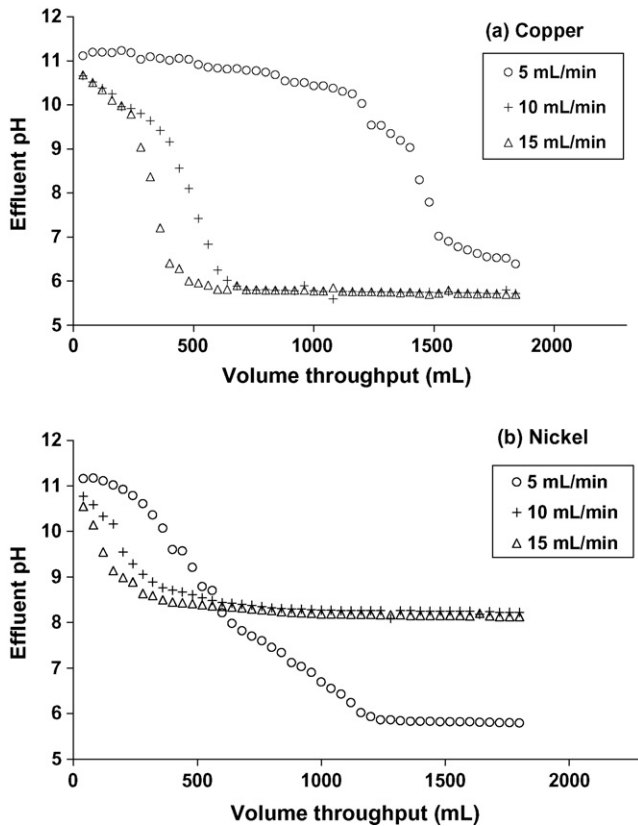


Fig. 4. Effect of influent flow rate on effluent pH for (a) Cu^{2+} and (b) Ni^{2+} .

essentially affected the H^+ ion concentration and that if the experiment were to run for a long enough time, the effluent pH would be the same as the influent value.

Fig. 5 shows the effect of influent flowrate on breakthrough curves for Cu^{2+} and Ni^{2+} on 8.41 wt% PEI/AC. Increasing the flow rate from 5 to 15 mL/min clearly shift the breakthrough curves from right to left indicating decreased service time of fixed bed. Breakthrough points for Cu^{2+} adsorption occur at volume throughputs of approximately 1440 mL (5 mL/min), 600 mL (10 mL/min) and 400 mL (15 mL/min) while for Ni^{2+} adsorption, breakthrough points occur at approximately 320 (5 mL/min), 120 (10 mL/min) and 80 mL (15 mL/min). The time required to reach breakthrough point is also observed to decrease with increase in flow rate. This effect is most likely attributed to the decrease in the residence time of the metal ions in the bed at higher flow rates. It is also observed that sharper breakthrough curves for adsorption of Cu^{2+} on PEI-impregnated AC are obtained at higher flow rates. This indicates higher intraparticle diffusion effect and a smaller transfer zone at higher flow rates [16]. The breakthrough volume and the quantity of metal ions adsorbed also decrease with increasing flow rate. This is due to the reduced contact time causing a weak distribution of the liquid inside the column, which leads to a lower diffusivity of the solute among the particles of the adsorbent [17]. Singh and Pant [18] explained that the decrease of breakthrough capacity of adsorbent due to increase in flow rate was caused by breakage of adsorption film surrounding adsorbent particles thereby reducing the adhesion of adsorbate to the adsorbent particle.

3.4. Modelling of breakthrough curves

In order to facilitate the design of adsorption column with PEI-impregnated AC as the fixed-bed material, prediction of break-

through curve for effluent is desirable. As such, it is necessary to fit the adsorption data using established models and subsequently determine salient parameters associated with these models to determine their influence for optimization of the fixed-bed adsorption process. Modelling of the breakthrough curves was carried out using three established models, namely, bed-depth-service-time (BDST), Thomas and Yoon–Nelson models.

The BDST model which was formulated by Hutchins [19] elucidates a relation between the service time and the packed-bed depth of the column [17] and is expressed as

$$C_0 t = \frac{N_0 h}{u} - \frac{1}{K} \ln \left[\frac{C_0}{C_t} - 1 \right] \quad (1)$$

where C_0 is the influent concentration (mmol/L), C_t is the effluent concentration at time t (mmol/L), K is the adsorption rate constant (L/(mmol min)), N_0 is the adsorption capacity (mmol/L), h is the bed depth of fixed-bed activated carbon (cm), u is the linear flow rate (cm/min) and t is the service time to breakthrough (min). A linear plot of $C_0 t$ against $\ln[(C_0/C_t) - 1]$ was employed to determine values of N_0 and K from the intercept and slope of the plot.

The Thomas model which was formulated by Thomas [20] determines the maximum solid phase concentration of solute on the adsorbent and the adsorption rate constant for an adsorption column. The linearized form of the model is expressed as

$$\ln \left[\frac{C_0}{C_t} - 1 \right] = \frac{k_{\text{Th}} q_0 m}{Q} - \frac{k_{\text{Th}} C_0 V_{\text{eff}}}{Q} \quad (2)$$

where k_{Th} is the Thomas rate constant (mL/(min mmol)), q_0 is the equilibrium Cu^{2+} or Ni^{2+} uptake per gram of the adsorbent (mmol/g), Q is the volumetric flow rate (mL/min), V_{eff} is the volume of effluent (mL) and m is the amount of adsorbent in the column (g). A linear plot of $\ln[(C_0/C_t) - 1]$ against V_{eff}/Q (or t) was employed

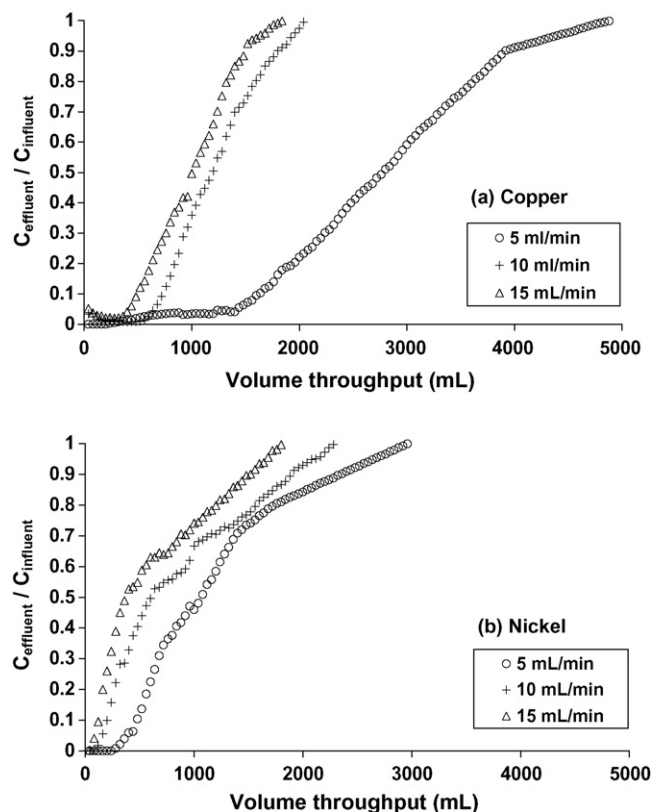


Fig. 5. Effect of influent flow rate on breakthrough curves of adsorption of (a) Cu^{2+} and (b) Ni^{2+} on 8.41 wt% PEI/AC (influent pH 5).

Table 2
BDST model parameters for fixed-bed adsorption of Cu²⁺ and Ni²⁺ on virgin and PEI-impregnated AC at 25 °C

| Activated carbon | Metal ion | Flow rate (mL/min) | <i>u</i> (cm/min) | Breakthrough time <i>t_b</i> (min) | <i>K</i> (L/mmol min) | <i>N₀</i> (mmol/L) | <i>R</i> ² -values | <i>ε</i> (%) |
|------------------|------------------|--------------------|-------------------|--|-----------------------|-------------------------------|-------------------------------|--------------|
| Virgin | Cu ²⁺ | 5 | 1.591 | 110.5 | 0.0350 | 55.2979 | 0.9830 | 9.81 |
| | Ni ²⁺ | 5 | 1.591 | 32.5 | 0.0221 | 38.3033 | 0.9030 | 9.15 |
| 8.41 wt% PEI/AC | Cu ²⁺ | 5 | 1.591 | 234 | 0.0120 | 118.3000 | 0.9804 | 1.45 |
| | Ni ²⁺ | 5 | 1.591 | 52 | 0.0166 | 55.0566 | 0.8988 | 7.87 |
| | Cu ²⁺ | 10 | 3.183 | 54 | 0.0526 | 59.2781 | 0.9514 | 10.49 |
| | Ni ²⁺ | 10 | 3.183 | 10.8 | 0.0327 | 43.8586 | 0.8611 | 9.33 |
| | Cu ²⁺ | 15 | 4.774 | 23 | 0.0907 | 45.3530 | 0.9540 | 8.97 |
| | Ni ²⁺ | 15 | 4.774 | 4.6 | 0.0513 | 26.8768 | 0.8884 | 4.32 |
| 16.68 wt% PEI/AC | Cu ²⁺ | 5 | 1.591 | 143 | 0.0252 | 65.2177 | 0.9893 | 3.75 |
| | Ni ²⁺ | 5 | 1.591 | 26 | 0.0198 | 37.6165 | 0.8515 | 10.12 |

to determine values of *k_{Th}* and *q₀* from the intercept and slope of the plot.

The Yoon–Nelson model [21] is based on the assumption that the rate of decrease in the probability of adsorption for each adsorbate molecule is proportional to the probability of adsorbate adsorption and the probability of adsorbate breakthrough on the adsorbent [17]. This model was used to investigate the breakthrough behavior of adsorption of Cu²⁺ or Ni²⁺ on AC. The linearized model for a single component system is expressed as

$$\ln \frac{C_t}{C_0 - C_t} = k_{YN}t - \tau k_{YN} \quad (3)$$

where *k_{YN}* is the rate constant (per min) and *τ* is the time required for 50% adsorbate breakthrough (min). A linear plot of $\ln [C_t/(C_0 - C_t)]$ against sampling time (*t*) was employed to determine values of *k_{YN}* and *τ* from the intercept and slope of the plot.

It is important to note that all the three models are mathematically equivalent in which a similar fitting equation can be obtained from Eqs. (1)–(3). This fitting equation is expressed as

$$\ln \left[\frac{C_0}{C_t} - 1 \right] = a - bt \quad (4)$$

where $a = KN_0h/u$ (BDST model), $k_{Th}q_0m/Q$ (Thomas model) or τk_{YN} (Yoon–Nelson model) while $b = KC_0$ (BDST model), $k_{Th}C_0$ (Thomas model) or k_{YN} (Yoon–Nelson model).

The average percentage errors (*ε*%) are used to indicate the fit between the experimental and theoretical values of *C_t/C₀* used for plotting breakthrough curves and they are calculated using in accordance to the following equation [22]:

$$\varepsilon = \frac{\sum_{i=1}^N [(C_t/C_0)_{exp} - (C_t/C_0)_{theo}] / (C_t/C_0)_{exp}}{N} \times 100 \quad (5)$$

where *N* is the number of measurements.

Tables 2–4 present the values of respective BDST, Thomas and Yoon–Nelson model parameters obtained from slopes and intercepts of linear plots. Analysis of *R*²-values indicates that the Cu²⁺ adsorption data fit the BDST, Thomas and Yoon–Nelson models very well as compared to the Ni²⁺ adsorption data. This indicates that all three models are valid for the application of adsorption of Cu²⁺ on both virgin and PEI-impregnated AC while it is conversely true for Ni²⁺. It is obvious that increases in flow rate result in decreases of *N₀*, *q₀* and *τ* and increases of *K*, *k_{Th}* and *k_{YN}* values. This trend indicates that external mass transfer which dominates the overall system kinetics occurs in the initial part of the adsorption process [17].

Table 3
Thomas model parameters for fixed-bed adsorption of Cu²⁺ and Ni²⁺ on virgin and PEI-impregnated AC at 25 °C

| Activated carbon | Metal ion | Flow rate (mL/min) | Breakthrough time, <i>t_b</i> (min) | <i>k_{Th}</i> (mL/(min mmol)) | (<i>q₀</i>) _{cal} (mmol/g) | (<i>q₀</i>) _{exp} (mmol/g) | <i>R</i> ² -values | <i>ε</i> (%) |
|------------------|------------------|--------------------|---|---------------------------------------|--|--|-------------------------------|--------------|
| Virgin | Cu ²⁺ | 5 | 110.5 | 34.40 | 0.1231 | 0.1503 | 0.9830 | 7.62 |
| | Ni ²⁺ | 5 | 32.5 | 20.00 | 0.0824 | 0.1004 | 0.9030 | 4.88 |
| 8.41 wt% PEI/AC | Cu ²⁺ | 5 | 234 | 11.80 | 0.2410 | 0.2974 | 0.9804 | 0.27 |
| | Ni ²⁺ | 5 | 52 | 14.90 | 0.1087 | 0.1274 | 0.8988 | 2.10 |
| | Cu ²⁺ | 10 | 54 | 51.70 | 0.1211 | 0.1293 | 0.9466 | 11.72 |
| | Ni ²⁺ | 10 | 10.8 | 28.20 | 0.0850 | 0.0919 | 0.8611 | 6.61 |
| | Cu ²⁺ | 15 | 23 | 87.00 | 0.0919 | 0.1059 | 0.9555 | 4.75 |
| | Ni ²⁺ | 15 | 4.6 | 45.60 | 0.0503 | 0.0667 | 0.8884 | 1.38 |
| 16.68 wt% PEI/AC | Cu ²⁺ | 5 | 143 | 24.30 | 0.1240 | 0.1505 | 0.9900 | 3.48 |
| | Ni ²⁺ | 5 | 26 | 16.80 | 0.0671 | 0.0806 | 0.8515 | 6.39 |

Table 4
Yoon–Nelson model parameters for fixed-bed adsorption of Cu²⁺ and Ni²⁺ on virgin and PEI-impregnated AC at 25 °C

| Activated carbon | Metal ion | Flow rate (mL/min) | Breakthrough time, <i>t_b</i> (min) | <i>k_{YN}</i> (per min) | <i>τ_{cal}</i> (min) | <i>τ_{exp}</i> (min) | <i>R</i> ² -values | <i>ε</i> (%) |
|------------------|------------------|--------------------|---|---------------------------------|------------------------------|------------------------------|-------------------------------|--------------|
| Virgin | Cu ²⁺ | 5 | 110.5 | 0.0344 | 208.74 | 211.00 | 0.9830 | 7.63 |
| | Ni ²⁺ | 5 | 32.5 | 0.0200 | 139.81 | 128.70 | 0.9030 | 4.94 |
| 8.41 wt% PEI/AC | Cu ²⁺ | 5 | 234 | 0.0118 | 447.07 | 450.20 | 0.9804 | 0.27 |
| | Ni ²⁺ | 5 | 52 | 0.0149 | 201.62 | 174.50 | 0.8988 | 2.09 |
| | Cu ²⁺ | 10 | 54 | 0.0517 | 112.28 | 107.10 | 0.9466 | 11.88 |
| | Ni ²⁺ | 10 | 10.8 | 0.0282 | 78.86 | 55.70 | 0.8611 | 6.63 |
| | Cu ²⁺ | 15 | 23 | 0.0873 | 56.92 | 58.00 | 0.9571 | 5.43 |
| | Ni ²⁺ | 15 | 4.6 | 0.0472 | 32.41 | 21.90 | 0.8737 | 2.88 |
| 16.68 wt% PEI/AC | Cu ²⁺ | 5 | 143 | 0.0249 | 245.59 | 247.50 | 0.9894 | 1.53 |
| | Ni ²⁺ | 5 | 26 | 0.0168 | 132.35 | 102.20 | 0.8515 | 6.36 |

It is also observed that the N_0 and q_0 values for Cu^{2+} and Ni^{2+} adsorption for 8.41 wt% PEI/AC are higher than that of virgin and 16.68 wt% PEI/AC. This indicates the effectiveness of the PEI impregnation process on enhancing the metal adsorption capacity of AC in which 8.41 wt% PEI/AC has the highest Cu^{2+} and Ni^{2+} adsorption capacities among the three AC samples. As elucidated in our previous study [8], this enhancement is most probably due to enhanced metal complexation effect provided by the presence of PEI molecules on the surface of AC which at the same time is sufficiently low to prevent excessive clogging of pores. It is surmised that the amount PEI impregnated for 16.68 wt% PEI/AC is rather excessive resulting in relatively more clogging of pores as evident in reduced surface area and total pore volume. As such, this clogging effect overwhelms the enhancing effect of complexation resulting in reduced Cu^{2+} and Ni^{2+} adsorption capacities for 16.68 wt% PEI/AC.

The Ni^{2+} adsorption capacity appears to be lower than that of Cu^{2+} for the same PEI-impregnated AC and similar operating conditions. The binding constant of metal–PEI complex, K_b , can be used to explain this observation. The value of K_b for Cu–PEI is higher than Ni–PEI irrespective of the types of aqueous media which indicates that Cu–PEI complex is more stable than Ni–PEI complex [15]. This implies that higher stability of Cu–PEI complexes and hence enhanced Cu^{2+} adsorption capacity.

3.5. Comparison of experimental and modelled breakthrough curves

The experimental and modelled breakthrough curves are shown in Figs. 6 and 7. For Cu^{2+} adsorption at flow rate of 5 mL/min, overlapping of the three models is observed and all the models are in very good agreement with the experimental curves. This indicates the applicability of all three models in predicting the fixed-bed Cu^{2+}

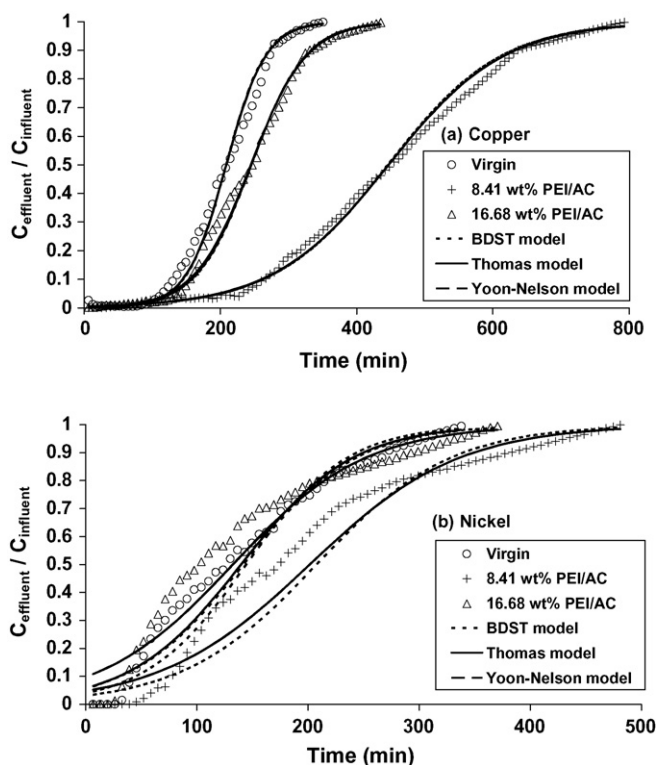


Fig. 6. Experimental and modelled breakthrough curves of adsorption of (a) Cu^{2+} and (b) Ni^{2+} on virgin and PEI-impregnated AC at influent pH 5 and flow rate 5 mL/min.

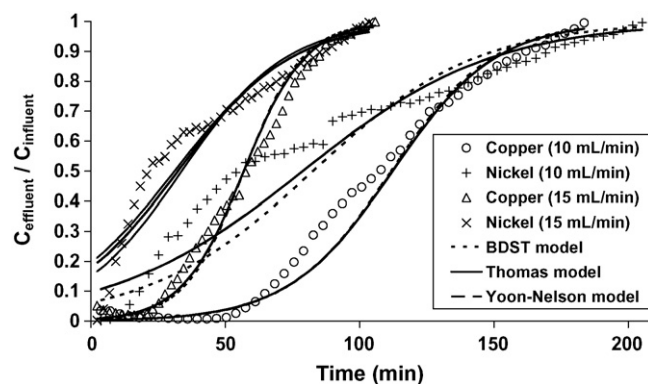


Fig. 7. Experimental and modelled breakthrough curves of adsorption of Cu^{2+} and Ni^{2+} on 8.41 wt% PEI/AC at flow rates 10 and 15 mL/min (influent pH 5).

adsorption behaviour of virgin and PEI-impregnated AC and thus, is useful for optimization of such fixed-bed adsorption processes. In contrast, the modelled curves of Ni^{2+} adsorption at all flow rates are in relative disagreement with the experimental curves except at the end of the breakthrough curves.

4. Conclusions

PEI impregnation at 8.41 wt% had increased the breakthrough volume and service time of AC by factors of 2.1 (Cu^{2+}) and 1.6 (Ni^{2+}). The PEI impregnation process enhanced the metal adsorption capacity of AC in which 8.41 wt% PEI/AC had the highest Cu^{2+} and Ni^{2+} adsorption capacities as compared to virgin and 16.68 wt% PEI/AC. This enhancement was due to enhanced metal complexation effect provided by the presence of PEI molecules on the surface of AC which at the same time was sufficiently low to prevent excessive clogging of pores. For Cu^{2+} adsorption, the modelled BDST, Thomas and Yoon–Nelson curves are in very good agreement with the experimental curves. This indicates the applicability of all three models in predicting the fixed-bed Cu^{2+} adsorption behaviour of virgin and PEI-impregnated AC. However, the modelled curves of Ni^{2+} adsorption were in relative disagreement with the experimental curves except at the end of the breakthrough curves.

Acknowledgements

The authors gratefully acknowledge the Ministry of Science, Technology and Innovation, Malaysia for the IRPA research grant and Bravo Green Sdn Bhd, Kuching, Malaysia for generous provision of palm shell activated carbon for research purposes. The authors would also like to acknowledge Mr. Mohd Jindra Aris for his assistance.

References

- J.P. Chen, X.Y. Wang, Removing copper, zinc and lead ion by granular activated carbon in pretreated fixed-bed columns, *Sep. Purif. Technol.* 19 (2000) 157–167.
- L. Monser, N. Adhoum, Modified activated carbon for the removal of copper, zinc, chromium and cyanide from wastewater, *Sep. Purif. Technol.* 26 (2002) 137–146.
- U.F.M. Ali, M.K. Aroua, W.M.A.W. Daud, Modification of a granular palm shell based activated carbon by acid pre-treatment for enhancement of copper adsorption, in: *Proceedings of the Third Technical Postgraduate Symposium (TECHPOS'04)* 15–16 December, Kuala Lumpur, Malaysia, 2004, pp. 75–79.
- Y.F. Jia, K.M. Thomas, Adsorption of cadmium ions on oxygen surface sites in activated carbon, *Langmuir* 16 (2000) 1114–1122.
- S.J. Vladimir, D. Malik, Characterization and metal sorptive properties of oxidized active carbon, *J. Colloid Interf. Sci.* 250 (2002) 213–220.
- S.J. Park, Y.S. Jang, Pore structure and surface properties of chemically modified activated carbons for adsorption mechanism and rate of Cr(IV), *J. Colloid Interf. Sci.* 249 (2002) 458–463.

- [7] D. Mugisidi, A. Ranaldo, J.W. Soedarsono, M. Hikam, Modification of activated carbon using sodium acetate and its regeneration using sodium hydroxide for the adsorption of copper from aqueous solution, *Carbon* 45 (2007) 1081–1084.
- [8] C.Y. Yin, M.K. Aroua, W.M.A.W. Daud, Impregnation of palm shell activated carbon with polyethyleneimine and its effects on Cd²⁺ adsorption, *Colloids Surf. A* 307 (2007) 128–136.
- [9] G. Issabayeva, Adsorption and electroreduction of copper and lead ions on palm shell activated carbon, Ph.D. Thesis, University of Malaya, Malaysia, 2005.
- [10] Department of Environment (DOE), Malaysian Environmental Quality Report, ISSN 0127-6433, 2002.
- [11] J.W. Schurer, P.H.J. Hoedemaeker, I. Molenaar, Polyethyleneimine as tracer particle for (immuno) electron microscopy, *J. Histochem. Cytochem.* 25 (1977) 384–387.
- [12] J.P. Chen, J.T. Yoon, S. Yiacoumi, Effects of chemical and physical properties of influent on copper sorption onto activated carbon fixed-bed columns, *Carbon* 41 (2003) 1635–1644.
- [13] S.Y. Quek, B. Al-Duri, Application of film-pore diffusion model for the adsorption of metal ions on coir in a fixed-bed column, *Chem. Eng. Process* 46 (2007) 477–485.
- [14] J.P. Chen, L. Wang, Characterization of metal adsorption kinetic properties in batch and fixed-bed reactors, *Chemosphere* 54 (2004) 397–404.
- [15] R.S. Juang, M.N. Chen, Measurement of binding constants of poly(ethylenimine) with metal ions and metal chelates in aqueous media by ultrafiltration, *Ind. Eng. Chem. Res.* 35 (1996) 1935–1943.
- [16] V. Brauch, E.U. Schlunder, The scale-up of activated carbon columns for water purification, based on results from batch tests, *Chem. Eng. Sci.* 30 (1975) 539–548.
- [17] S. Kundu, A.K. Gupta, As(III) removal from aqueous medium in fixed bed using iron oxide-coated cement (IOCC): experimental and modeling studies, *Chem. Eng. J.* 129 (2007) 123–131.
- [18] T.S. Singh, K.K. Pant, Experimental and modelling studies on fixed bed adsorption of As(III) ions from aqueous solution, *Sep. Purif. Technol.* 48 (2006) 288–296.
- [19] R.A. Hutchins, New simplified design of activated carbon system, *Am. J. Chem. Eng.* 80 (1973) 133–138.
- [20] H.C. Thomas, Heterogeneous ion exchange in a flowing system, *J. Am. Chem. Soc.* 66 (1944) 1664–1666.
- [21] Y.H. Yoon, J.H. Nelson, Application of gas adsorption kinetics. Part 1. A theoretical model for respirator cartridge service time, *Am. Ind. Hyg. Assoc. J.* 45 (1984) 509–516.
- [22] E. Malkoc, Y. Nuhoglu, Y. Abali, Cr(VI) adsorption by waste acorn of *Quercus ithaburensis* in fixed beds: prediction of breakthrough curves, *Chem. Eng. J.* 119 (2006) 61–68.